Pergamon

0042-6989(95)00103-4

Vision Res. Vol. 36, No. 3, pp. 373–390, 1996

0042-6989/96 $15.00 + 0.00

Mechanisms Underlying the Detection of Increments in Parafoveal Retina

WAYNE VERDON,*† GUNILLA HAEGERSTROM-PORTNOY*

Received 4 March 1992; in revised form 8 July 1994; in final form 21 March 1995

It is well established that the spectral sensitivity under photopic conditions varies across the human retina. We investigate the mechanisms underlying these spectral changes. Through the use of color appearance, flicker sensitivity, additivity, discrimination at threshold and modeling, we show that the changes in spectral sensitivity on a photopic white background across parafoveal retina are consistent with shifts in cone weightings to (L–M) and (M–L) chromatic channels. This two channel model, developed to account for foveal spectral sensitivity curves (Sperling & Harwerth, 1971 *Science, 172,* 180–184), provides a better description of parafoveal data than both a single color channel upper envelope model (comprised of a single red–green opponent channel and an achromatic mechanism) and a vector model (combining a red–green opponent channel with an achromatic component). Thus while the two channel model ([L–M] and [M–L]) of foveal color vision is generalizable to the parafovea, simple models with a unitary red/green process are not. Although the two channel model can accurately fit parafoveal spectral sensitivity curves without it, a small contribution from a luminance mechanism might improve the ability of the two channel model to account for threshold discrimination and additivity data.

Opponent Luminance Spectral sensitivity Color Increment threshold

INTRODUCTION

Separate chromatic and luminance channels have been identified psychophysically in human vision. Chromatic (color opponent) channels detect a test light of relatively large size and long duration when presented on a white background, whereas the luminance (non-opponent, achromatic) channel is more likely to detect a small, short duration test light or one that is flickering at a high frequency (King-Smith & Carden, 1976; King-Smith, 1975). Presenting the stimulus away from the fovea appears to bias against detection by chromatic channels. For example, the detection mechanism for a 1 deg diameter test light at the fovea has a three peaked spectral shape, but at 20 deg retinal eccentricity the curve is unimodal (Kuyk, 1982; Krastel, Jaeger, Zimmermann, Heckmann & Krystek, 1991). The shape of the peripheral spectral sensitivity is more characteristic of detection by a luminance mechanism because the single peak occurs at about 555 nm and the curve resembles the CIE photopic luminosity function, $V(\lambda)$ (Kuyk, 1982). In fact, a test light of approximately 4 deg diameter is needed at 20 deg eccentricity to regain a spectral sensitivity curve similar to the foveal curve measured with a 1 deg diameter test light. Similarly, enlarging the stimulus in peripheral retina is necessary to achieve foveal-like performance for other color vision tasks including wavelength discrimination (van Esch, Koldenhof, van Doorn & Koenderink, 1984), color appearance (Gordon & Abramov, 1977; Abramov, Gordon & Chan, 1991) and color detection thresholds (Johnson & Massof, 1982; Johnson, 1986).

We sought to determine the causes of the changes in spectral sensitivity on a white background as a small test light is presented at increasing eccentricities across the parafoveal retina. It is well established that the spectral sensitivity measured for foveal test lights on a white background, reflects color opponent (post-receptoral) processing. Also, it is known that over the central few degrees the ratio of M (middle wavelength sensitive) to L (long wavelength sensitive) cones remains the same (Nerger & Cicerone, 1992), and the spectral absorption of each cone type is independent of retinal position. Therefore shifts in spectral shape at different retinal positions reflect changes in post-receptoral signal processing.

To bias towards detection by chromatic channels the test stimulus was filtered to remove high spatial and temporal frequencies. The stimulus is similar to the low frequency test of Thornton and Pugh (1983a). Spectral sensitivities from 501 to 680 nm were measured at 0, 1, 2, 3, 4 and 5 deg eccentricity. We asked whether a relative increase in the sensitivity of a luminance mechanism is responsible for the change in spectral shape across the parafovea, as previously suggested, and also which, if any, model of foveal color vision can best

*School of Optometry, University of California at Berkeley, CA 94720-2020, U.S.A. [*Fax* +1-510-643-5109; *Email* verdon@mindseye.berkeley.edu].
†To whom all correspondence should be addressed.

account for the parafoveal data. Two upper envelope models previously applied to foveal data were applied to our parafoveal data. The first has independent luminance and chromatic mechanisms (e.g. Thornton & Pugh, 1983a). The second model uses one color mechanism, M–L, to model sensitivity at wavelengths shorter than that at which Sloan's notch occurs (approximately 580 nm), and another color mechanism, L–M, to model sensitivity at wavelengths longer than Sloan's notch. There is no independent luminance mechanism in the original version of this model (e.g. Sperling & Harwerth, 1971). We also consider a vector model in which signals from a single red–green chromatic mechanism combine with luminance signals. Using curve fitting, additivity, flicker sensitivity, and color discrimination at threshold we determined that chromatic mechanisms contribute to detection across the spectrum, despite a unimodal spectral curve at 5 deg eccentricity. Therefore simple shifts in the relative sensitivities of independent luminance and chromatic mechanisms alone cannot account for the data. The vector model systematically underestimates sensitivity extrafoveally in the middle of the spectrum. The two channel opponent model [(L–M) and (M–L)] is the simplest model consistent with the additivity and color discrimination data, and it provides an excellent fit to the spectral data at all eccentricities. Our analysis suggests that the changes in spectral sensitivity with eccentricity are consistent with changes in cone weightings to the (M–L) and (L–M) opponent channels, with the excitatory component of each channel becoming more dominant with increased eccentricity. Using this model it is unnecessary to invoke achromatic mechanisms in detection, although our data do not preclude more than two active mechanisms near threshold, one of which might be an achromatic mechanism. In fact this might help explain the small (approximately 0.2 log unit) discrepancy between detection and discrimination at some wavelengths. A unitary red–green mechanism provides a worse account of the parafoveal changes in spectral sensitivity whether considered in an upper envelope model or a vector model.

METHODS

All experiments were performed on a 2 source, 4 channel Maxwellian view optical system. The sources were 150 W, 15 V Tungsten–Halogen bulbs (Osram) run from a Sorensen ACR 3000 regulated power supply. The bulbs were run at 13.8 V to maximize bulb life. Spectral light was provided by 3-cavity interference filters (Ealing Electro-Optics) with half-height bandwidths ranging from 7.4 to 12.3 nm (mean = 9.6 nm). Light levels were controlled by circular Kodak Inconel neutral density wedges and auxiliary reflective neutral density filters. Head position was maintained using a dental impression bite bar mounted on an XYZ stage. Stimuli were viewed through a Lewis achromatizing lens (Lewis, Katz & Oehrlein, 1982) to correct the eye's longitudinal chromatic aberration. The final image of the source filament measured 2 mm. The optical system was run from an Apple IIe microcomputer.

Light levels were measured with a Spectra Pritchard Photometer (Model 1980A) using Westheimer's technique (Westheimer, 1966). Interference filters were calibrated in place radiometrically with a United Detector Technology radiometer and a Pin 10-DP photodiode. Daily light output of each source was monitored with the same photodiode placed in a collimated beam.

For the spectral sensitivity measurements, the test and background lights were derived from the same source. Two linear polarizing filters were placed in the test channel. One was fixed and the other mounted on a stepper motor to allow the test to be temporally ramped on and off. For the additivity experiments, the 2 channels comprising the test were first combined in various ratios (see below) and then passed through the 2 polarizing filters.

Stimulus

The background was 3.55 log td Tungsten–Halogen white. The aperture defining the test subtended 26 min arc diameter when in the focal plane of the Maxwellian lens, but for the experiments it was moved to create 2.50 diopters of defocus. This resulted in a spot approximately 35 min arc diameter. Its temporal waveform was a single cycle sinusoid of 1.67 Hz (600 msec trough-to-trough). The test was presented at the fovea and at 1, 2, 3, 4 and 5 deg eccentricity in the superior field of the right eye. Other than eccentricity and wavelength, no parameters were changed during these experiments. Fixation was guided by small spots engraved on a glass slide inserted in the background beam.

Subjects

Two subjects participated in these experiments, SH and author WV. SH was naive to the purpose of the experiments. Both are experienced observers, and have normal color vision by the Nagel anomaloscope, Farnsworth–Munsell 100 hue test and standard book tests.

Methods

Spectral increment thresholds were measured using the method of adjustment with a step size of 0.08 log unit. Wavelengths were chosen in random order from 500 to 680 nm in 10 nm intervals. Foveal and 5 deg spectral sensitivities for WV were measured 5 and 4 times, respectively, on different days. All other spectral sensitivities at other positions were measured at least twice on different days. For the flicker experiments (see Fig. 3) a sector wheel was rotated in the test channel to provide 35 Hz square wave flicker, within the low frequency envelope.

Additivity. For the additivity experiments, test wavelengths of 520 and 620 nm were chosen. We used the technique described by Guth, Donley and Marrocco (1969) and Drum (1982) to test for additivity. First, thresholds for each component alone were measured. The components were then presented in a ratio of 1:2,

1:1, and 2:1 and the threshold for the combination was determined. The amount of each component was plotted in threshold units. Thresholds were measured in a two alternative forced choice technique using 2 randomly interleaved staircases. One staircase began above threshold while the other began below threshold (the initial threshold was approximated by the method of adjustment). The step size was fixed at 0.08 log unit. Three correct responses were required to make the staircase step to the next dimmer level and one incorrect response was need to step the staircase up. After 50 trials, all the responses were pooled to generate a psychometric function and threshold was determined by Probit analysis (Finney, 1947). A control experiment was run on WV at the fovea in which both components of the test mixture were 520 nm. As expected, additivity held at all 3 ratios of the components. In general, the additivity data do not fall precisely on diagonals with slopes 2, 1 and 0.5. This is because the nominal 0.3 ND filter used to attenuate each component (for ratios 1:2 and 2:1), did not exactly reduce radiance by a factor of two. Also, Probit analysis was done off-line which meant that a threshold unit of each component was estimated by the average of staircase reversals during the experimental run, and any difference between this value and the Probit estimate was corrected after the experiment.

Macular pigment. Individual measures of macular pigment density were made at the fovea and 1, 2, 3, 4 and 5 deg eccentricity. Measurements were made on the same apparatus as the main experiments using the same low frequency test. A flicker wheel was interposed in the test channel to give a 20 Hz square wave test in a low frequency envelope. Flicker detection thresholds were set using the method of adjustment. Test wavelengths of 460 and 631 nm were used because macular pigment absorbs maximally at the former wavelength and minimally at the latter. The stimulus was presented on a 2.83 photopic td 460 nm 10 deg field to eliminate contributions from rods and S cones and to help isolate L cones. We assumed zero optical density for macular pigment at 7 deg eccentricity. The difference in sensitivity to the 2 wavelengths was found at each eccentricity. The difference between this value and the value at 7 deg was taken as a measure of macular pigment density. Optical densities for SH at 0, 1, 2, 3 and 4 deg eccentricity were 0.38, 0.43, 0.10, 0, 0 log units (the higher density at 1 deg was repeatable on a different occasion using a different optical system and a 24 min diameter, 200 msec focused test flickering at 15 Hz). For WV they were 0.67, 0.38, 0.15, 0.05, 0.05 log units. Zero optical density was measured at 5 deg in both subjects.

Discrimination. Color discrimination at threshold was determined using a 2×2 temporal forced choice procedure (Watson & Robson, 1981; Mullen & Kulikowski, 1991). The subject was instructed to choose the interval in which the test was presented and to identify whether wavelength 1 or 2 was presented. Practice and feedback on discrimination were given. The method of constant stimuli was used with an intensity series in 0.1 log unit steps, spanning 0.9 log units centered around the approximate threshold. To avoid one light being more detectable than another, which could artifactually improve discrimination, the radiance of the most detectable light was reduced with a neutral density filter until both lights were equally detectable. There were approximately 14 trials at each of 7 intensity levels for WV and approximately 25 for SH. Psychometric functions were generated for detection and discrimination and fit by Probit functions (Finney, 1947).

Achromatic mechanism sensitivity. Two of the models we tested involved possible contributions from an achromatic mechanism. To avoid adding the achromatic mechanism as an unconstrained variable for modeling purposes, we measured its sensitivity using the low frequency test on a white background. A similar approach has been used by Kranda and King-Smith (1979). Threshold for the luminance mechanism was determined by method of adjustment using an achromatic low frequency test (slow white-on-white). We assume the slow white increment presented on the white background is detected by a luminance mechanism because there is no chromatic difference between test and background. However, a focussed red test flash on a red background is largely L cone detected despite the lack of chromatic contrast in the stimulus (Wandell, Sanchez & Quinn, 1982; Stromeyer, Kronauer & Cole, 1983), and while our stimulus is dissimilar, our assumption remains unproven. The white test was then flickered at 25 Hz (square wave) within the low frequency envelope, and a new *flicker* detection threshold measured (flicker white-on-white). Because chromatic mechanisms are unable to follow high frequency flicker (Kelly, 1983), this latter threshold is determined exclusively by a luminance mechanism, regardless of spectral content. We believe the difference between the slow white-on-white and the flicker white-on-white thresholds is due to the difference in temporal sensitivity of the luminance mechanism to the two white test lights, and to the fact that the flickering light is occluded by the flicker wheel for half the test duration. We further assume that the difference (in log units) between the slow white-on-white and the flicker white-on-white thresholds can be applied to a spectral test. The assumption is reasonable given the univariant nature of a luminance mechanism. Subject WV was more sensitive to the low frequency test by 0.18, 0.31, 0.30, 0.30, 0.28 and 0.31 log unit at the fovea, 1, 2, 3, 4 and 5 deg eccentricity. Subject SH was more sensitive to the low frequency test by 0.19 and 0.14 log unit at the fovea and 5 deg eccentricity respectively. Achromatic mechanism sensitivity was not measured on SH at 1, 2, 3 and 4 deg eccentricity. By measuring 25 Hz *flicker* detection thresholds at any chosen wavelength, we could apply the above correction factor for the appropriate eccentricity for each subject, and thereby determine the sensitivity of the luminance mechanism to the low frequency test. Flicker thresholds were measured at each eccentricity for 620 and 561 nm lights, and these thresholds were then corrected for the effects of the flicker. $V(\lambda)$ (corrected for macular pigment at each eccentricity) was placed to best fit these data.

Modeling

The data were fit by a least squares procedure using the Smith and Pokorny fundamentals (tabulated in Wyszecki & Stiles, 1982). The linear fundamentals were quantized and normalized prior to modeling. The fundamentals were adjusted according to each subject's macular pigment density at the eccentricity being tested. It was assumed that the Smith and Pokorny tabulated fundamentals contained 0.31 log unit macular pigment as this is the amount of macular pigment needed to be subtracted from the CIE 2 deg $V(\lambda)$ to match the CIE 10 deg $V_{10}(\lambda)$ (Wyszecki & Stiles, 1982) for wavelengths longer than 460 nm. The very close match of the CIE curves after macular pigment correction justified our assumption that the curves differed only due to macular pigment screening, in agreement with Stabell and Stabell (1984). We reasoned that the optical density of macular pigment should be the same in the average CIE 2 deg observer and the average observer used to determine the Smith and Pokorny L and M cone fundamentals.

Two upper envelope models were used. The first is a linearly subtractive model represented by:

$$\text{green peak}(\lambda = 500\text{–}570\text{ nm}) = k_1|M_\lambda - k_2 L_\lambda|;$$

$$\text{red peak}(\lambda = 580\text{–}660\text{ nm}) = k_3|M_\lambda - k_2 L_\lambda|;$$

$$\text{luminance} = [V(\lambda)].$$

where k_2 is a weighting coefficient that determines the cross point (Sloan's notch) of a single red–green channel. The resulting spectral curve has two peaks at approximately 535 and 610 nm, designated here as the green and red peaks. The green and red peaks of this model are treated independently after the weighting, i.e. they are each allowed to slide vertically on a $\log_{10}$ scale to best fit the data. Allowing independent adjustments to the green and red peaks adds two coefficients, k_1 and k_3. Thornton and Pugh (1983a) have shown that this model successfully fits foveal data measured with a stimulus similar to ours. It predicts a precipitous sensitivity loss at the cross point. Therefore, at extrafoveal loci for which the data show no deep notch, a second mechanism, either a luminance channel or a blue–yellow channel, must be introduced to detect the test. We measured the sensitivity of the luminance mechanism (see Methods) to allow it to be placed correctly with respect to the spectral data. This avoided adding a fourth coefficient to this model. In fitting the data, there is no practical difference in choosing between a luminance and a blue–yellow mechanism, because this final mechanism is needed to fit a few data points over which sensitivity is relatively constant. Extrafoveally the green peak was fit to wavelengths from 501 to 551 nm, and the red peak to wavelengths from 600 to 681 nm. This avoids the poor concordance between the model and the data in the notch region from upsetting the fits at all spectral locations. We refer to this as the single red–green channel model.

The second upper envelope model is that of Sperling and co-workers (Sperling & Harwerth, 1971; Kranda & King-Smith, 1979; Sperling, Wright & Mills, 1991). It is a two channel linear model, meaning that two red–green opponent channels are used to fit data over the long wavelength part of the spectrum. If sensitivity over the entire visible spectrum is measured, a short wave mechanism is needed, but we are concerned here only with wavelengths longer than 500 nm. The green and red peaks are fit by:

$$\text{green peak}(\lambda = 500\text{–}570\text{ nm}) = k_1|k_2 M_\lambda - L_\lambda|;$$

$$\text{red peak}(\lambda = 580\text{–}660\text{ nm}) = k_3|k_4 L_\lambda - M_\lambda|.$$

The model has 4 coefficients. A feature of this model is that it allows independent shape changes to the red and green peaks of the opponent function whereas the single channel model does not. This model successfully fits foveal spectral data, and changes to foveal spectral sensitivities due to chromatic adaptation (Sperling *et al.*, 1991). Note that this model is capable of fitting foveal data without using either a separate luminance mechanism or a blue–yellow color mechanism (Sperling & Harwerth, 1971; Kranda & King-Smith, 1979).

The third model applied is a vector model. Here we assume threshold is determined by a vector combination of signals from a luminance mechanism (with the shape of $V(\lambda)$ corrected individually for macular pigment at each eccentricity) and a single red–green channel as described above. This model is represented by:

$$\text{green peak}(\lambda = 500\text{–}570\text{ nm}) = [(V\lambda)^2 + k_1(k_2 L_\lambda - M_\lambda)^2]^{0.5};$$

$$\text{red peak}(\lambda = 580\text{–}660\text{ nm}) = [(V\lambda)^2 + k_3(k_2 L_\lambda - M_\lambda)^2]^{0.5}.$$

Without allowing independent adjustments of the red and green peaks, this model is incapable of simultaneously fitting both red and green peaks of the spectral sensitivities, as is the single channel model. The luminance mechanism sensitivity was measured for each subject under the appropriate experimental conditions (see Methods). We have not included a blue–yellow component to the vector model (in contrast to Guth, 1991) because there is little previous evidence that the yellow peak of a blue–yellow channel mediates detection of a spectral increment on a white field (Thornton & Pugh, 1983b; Kranda & King-Smith, 1979). In the foveal data of Thornton and Pugh (1983a) where marked red–green opponent interaction was demonstrated, there was no evidence of detection by a yellow mechanism, other than possibly at the low point of the notch. According to Thornton and Pugh (their Fig. 2A, 1983b), the peak of the yellow mechanism at the trough must be approximately 1.5 log units below that of the red and green peaks. We know of no evidence to suggest the yellow peak of the blue–yellow opponent mechanism sharply increases in sensitivity away from the fovea compared to the red–green mechanism, as would be required by the change in spectral sensitivity shown here. Furthermore, that part of the spectrum that appears yellow remains narrow parafoveally and this argues against a rising yellow peak. Vector models are usually applied to a diverse data set which includes color

perception and light adaptation, and for a unified model to account for this range of data, a blue–yellow component is needed (Guth, Massof & Benzschawel, 1980). We are concerned here with a more restricted data set.

RESULTS

Spectral sensitivities and modeling

Figure 1 shows foveal and 5 deg spectral sensitivities using the low frequency test on a white background for subject SH. Figure 2 shows the results for WV. For both subjects, the foveal data show two peaks at about 535 and 610 nm, with a notch at about 580 nm. This type of data has been reported previously (King-Smith & Carden, 1976; Thornton & Pugh, 1983a). The 5 deg and foveal spectral sensitivities clearly differ in shape. The notch has gone at 5 deg, leaving a single broad peak. To show that the spectral bandwidth of the foveal and 5 deg data is comparable, an L cone template (individually corrected for macular pigment) has been fit to the long wavelength slope of the data. We do not mean to imply that the template provides a satisfactory fit to any of the data here; it is presented to facilitate shape comparison. Wooten and Wald (1973) showed broadening of spectral sensitivities with eccentricity under chromatic adaptation conditions.

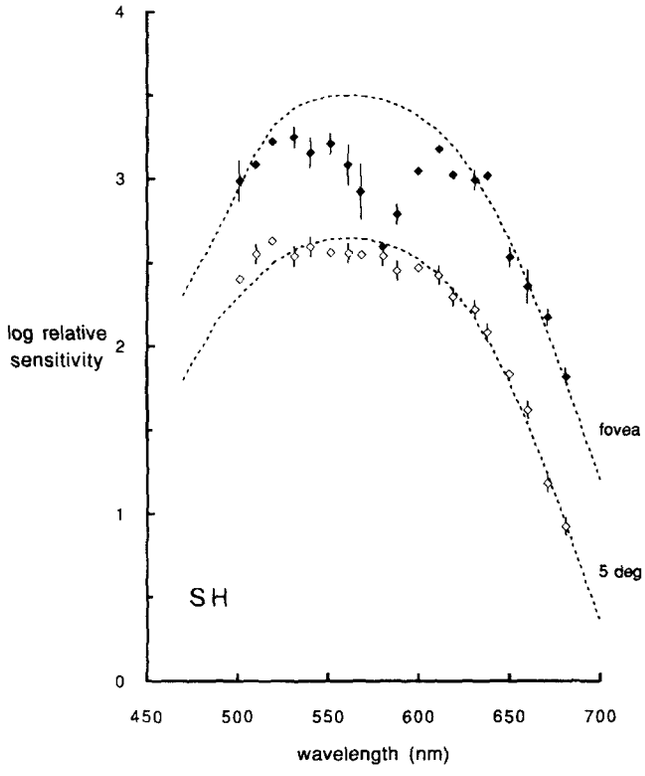

FIGURE 1. Spectral sensitivities for SH measured using the low frequency test on a white field at the fovea (solid symbols) and at 5 deg eccentricity (open symbols). Data are correctly placed relative to each other. The dotted line is the quantized Smith and Pokorny L cone fundamental (Wyszecki & Stiles, 1982) corrected for macular pigment and fit to the long wavelength slope of the data. It is plotted to allow shape and spectral bandwidth comparisons between the two data sets and is not considered a good fit to either curve. Zero on the ordinate corresponds to 11 $\log_{10}$ quanta·sec^{-1}·deg^2. At both locations, $n = 2$. Bars indicate full range of measurement.

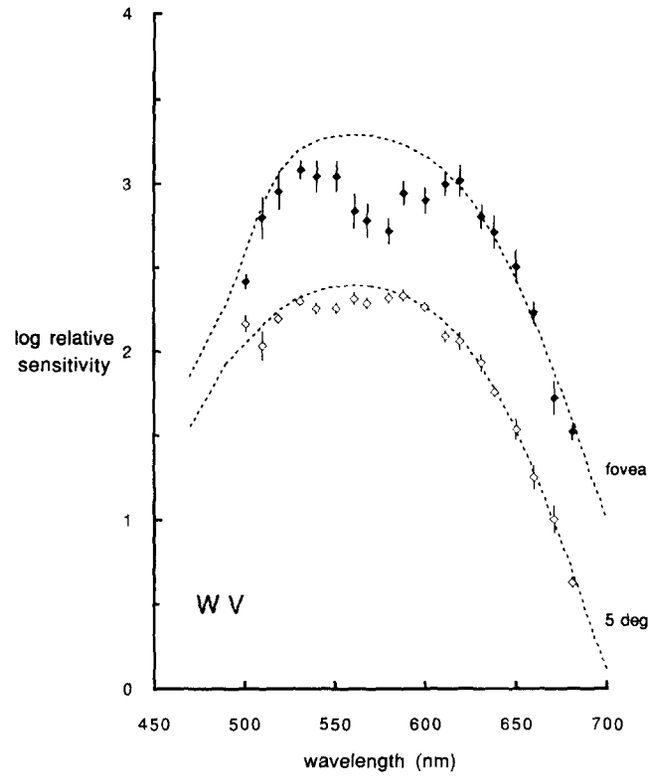

FIGURE 2. Spectral sensitivities for WV. Legend same as Fig. 1. At the fovea, $n = 5$, grand SD = ± 0.16 log unit. At 5 deg, $n = 4$, grand SD = ± 0.08 log unit. Bars indicate ± 1 SEM.

We measured 35 Hz flicker detection thresholds using the low frequency envelope, at 5 deg eccentricity. This was done to determine whether the spectral sensitivity curves at 5 deg in Figs 1 and 2 were the same spectral shape as a luminance mechanism measured at the same location. Also, if increment detection was mediated by L cones, as the test sensitivity might suggest, the detecting mechanism would be able to follow 35 Hz flicker and the test sensitivity should not change shape. Figure 3 (top), shows 35 Hz flicker detection thresholds for WV at 5 deg eccentricity. The quantized CIE 10 deg $V(\lambda)$ curve (Wyszecki & Stiles, 1982), with no correction for macular pigment, provides a good description of the data. $V_{10}(\lambda)$ is shown fit to the 5 deg increment threshold data for each subject, replotted from Figs 1 and 2. The fit to the 5 deg increment threshold spectral sensitivities is systematically poor indicating that detection is neither by a luminance mechanism nor by L cones.

Figure 4 shows spectral sensitivities from the fovea to 5 deg in 1 deg steps for SH. The data are fit with the 2 channel model. The notch becomes progressively less obvious with increased eccentricity and it disappears between 4 and 5 deg. However, up to that eccentricity the notch remains at approximately 570–580 nm. We therefore fit all data up to and including 570 nm with the green peak $k_1|k_2M_\lambda - L_\lambda|$ of the two channel opponent model, and data 580 nm and longer with the red peak $k_3|k_4L_\lambda - M_\lambda|$, even at those locations where the notch is not clearly defined. The same procedure was used to

fit the data of WV shown in Fig. 5. The model fits the longer wavelength data very well. The shorter wavelength data tend to be less smooth extrafoveally and the model fit is slightly worse. We have evidence from discrimination at threshold measures (below) that a blue mechanism is active away from the fovea in the region from about 500 to 520 nm, and thus fitting the first 2 or 3 data points with the green mechanism might be an oversimplification.

Figure 6 shows the fits of the single red–green channel model to the previously plotted data set for SH. The solid line is $V(\lambda)$, the photopic luminosity function, positioned at the fovea and 5 deg eccentricity according to independent measurement (see Methods). The single channel fits are worse than those of the two channel model at short wavelengths. Inspection reveals that the green and red peaks become broader on either side of the notch, effectively filling-in the notch. Simply making the notch shallower by fitting, for example, an achromatic mechanism does not capture this feature. The dashed line in the last panel shows the achromatic mechanism positioned to coincide with the threshold data over the center of the spectrum. The apparently good fit is misleading. The solid line in the last panel (Fig. 6) shows the true position of the achromatic mechanism at 5 deg,

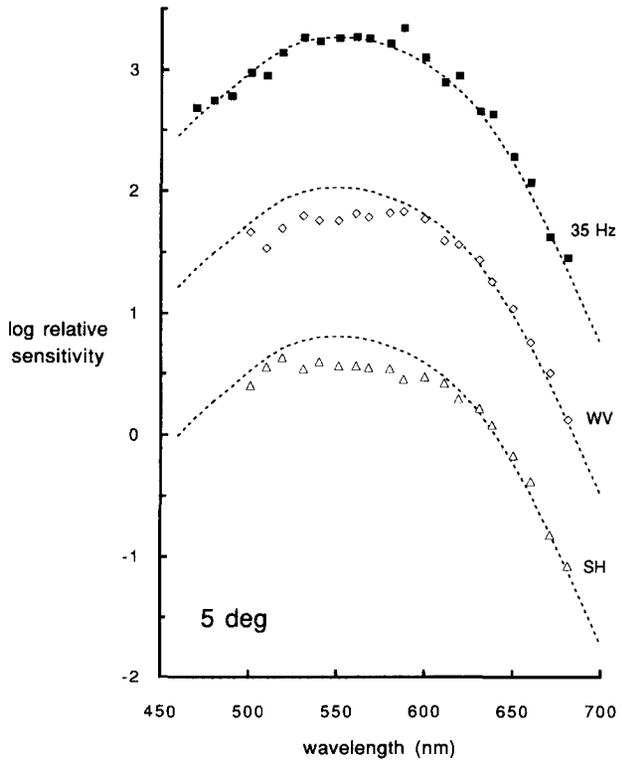

FIGURE 3. Spectral sensitivities measured at 5 deg eccentricity. The solid symbols show 35 Hz flicker detection thresholds for WV, and the open symbols show increment thresholds for SH and WV replotted from Figs 1 and 2. All dotted curves are the CIE $V_{10}(\lambda)$ (Wyszecki & Stiles, 1982). The good fit to the flicker data shows that the CIE curve is a reasonable approximation to a luminosity function at 5 deg, while the systematically poor fit to the increment threshold data shows that detection is by a different mechanism(s). For clarity, the flicker data are moved up 2 log units on the ordinate, and the curves for WV and SH are displaced down by 0.5 and 2 log units, respectively. Zero on the ordinate corresponds to 11 $\log_{10}$ quanta $\cdot$ sec^{-1} $\cdot$ deg^{2}.

determined by independent measurement. It lies 0.15 log unit below the threshold data in this region. Furthermore, fitting a wide (approximately 50 nm) spectral region with an achromatic mechanism implies that colors cannot be discriminated at threshold within this region. The results of the discrimination experiments described below contradict this implication, providing evidence against achromatic detection. The fit of the single channel model to data for WV are shown in Fig. 7. The solid line indicates the achromatic mechanism correctly positioned at each eccentricity. The fits show a small consistent error in the region of 580 to 620 nm. Furthermore in the center of the spectrum, the colored appearance of threshold lights and the ability to discriminate colors at or very close to threshold argues that chromatic mechanisms are active. This is in contrast to the model's implied precipitous chromatic sensitivity loss near the spectral cross point of a single red/green mechanism.

Table 1 shows the coefficients used to fit the one channel and two channel models for both subjects.

In Fig. 8, we show the M and L cone weightings for the green and red peaks of the two channel model, plotted against eccentricity. At the fovea, L and M cones are weighted approximately equally to best fit the red peak, and M cones are weighted twice as heavily as L cones to fit the green peak. As eccentricity increases, the excitatory cone weightings increase. This means the green peak becomes more heavily dominated by M cones, and the red peak by L cones. Thus, the notch fills in and the spectral sensitivity becomes less opponent looking. M and L cone weightings increase on average by a factor of 2.4 and 3.5 respectively, from the fovea to 5 deg eccentricity. As mentioned above, the change in weightings must reflect postreceptoral processes as the relative numbers of L and M cones remains approximately constant with eccentricity.

Figures 9 and 10 show fits of the vector model to the data of WV (fovea through 5 deg) and SH (fovea and 5 deg only). The solid line is $V(\lambda)$ correctly positioned by measurement. The dotted line is the best fit vector model ($k_2 = 0.65$). The model fits the spectral extremes well. At approximately 580 nm the sensitivity of the red–green component drops sharply and it no longer contributes significantly to detection. The peak sensitivity of the achromatic mechanism is at 555 nm, and there is a spectral region from approximately 570–600 nm, where the sensitivities of both mechanisms are relatively low. The vector model consistently underestimates sensitivity in this region, resulting in a systematically poor fit that is evident for both observers.

Color discrimination at thresholds

At all eccentricities both subjects perceived color at detection threshold, or very slightly above it. This is a sign of detection by opponent mechanisms and it was quantified by measuring discrimination at detection threshold. Two issues can be resolved by these experiments. First, in the critical region of the notch, are opponent mechanisms more sensitive than

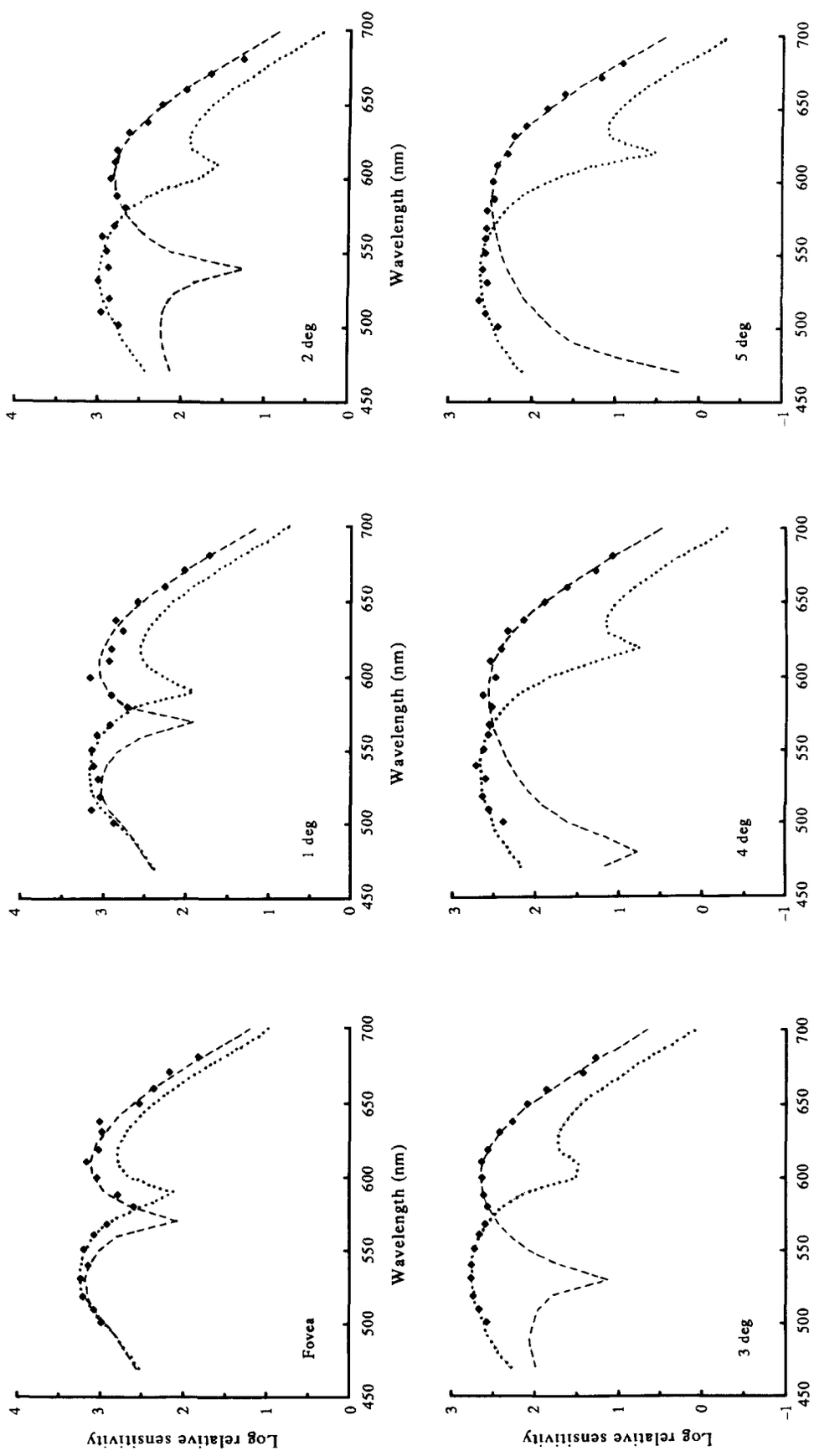

FIGURE 4. Spectral sensitivities for SH measured using the low frequency test on a white field at eccentricities from the fovea to 5 deg. The data are fit by the two channel model. The middle wavelength (green) peak is fit by $k_1|k_2M_z - L_z|$ (dotted line), and the long wavelength (red) peak is fit by $k_3|k_4L_z - Mz|$ (dashed line). The model describes the data well at all retinal positions.

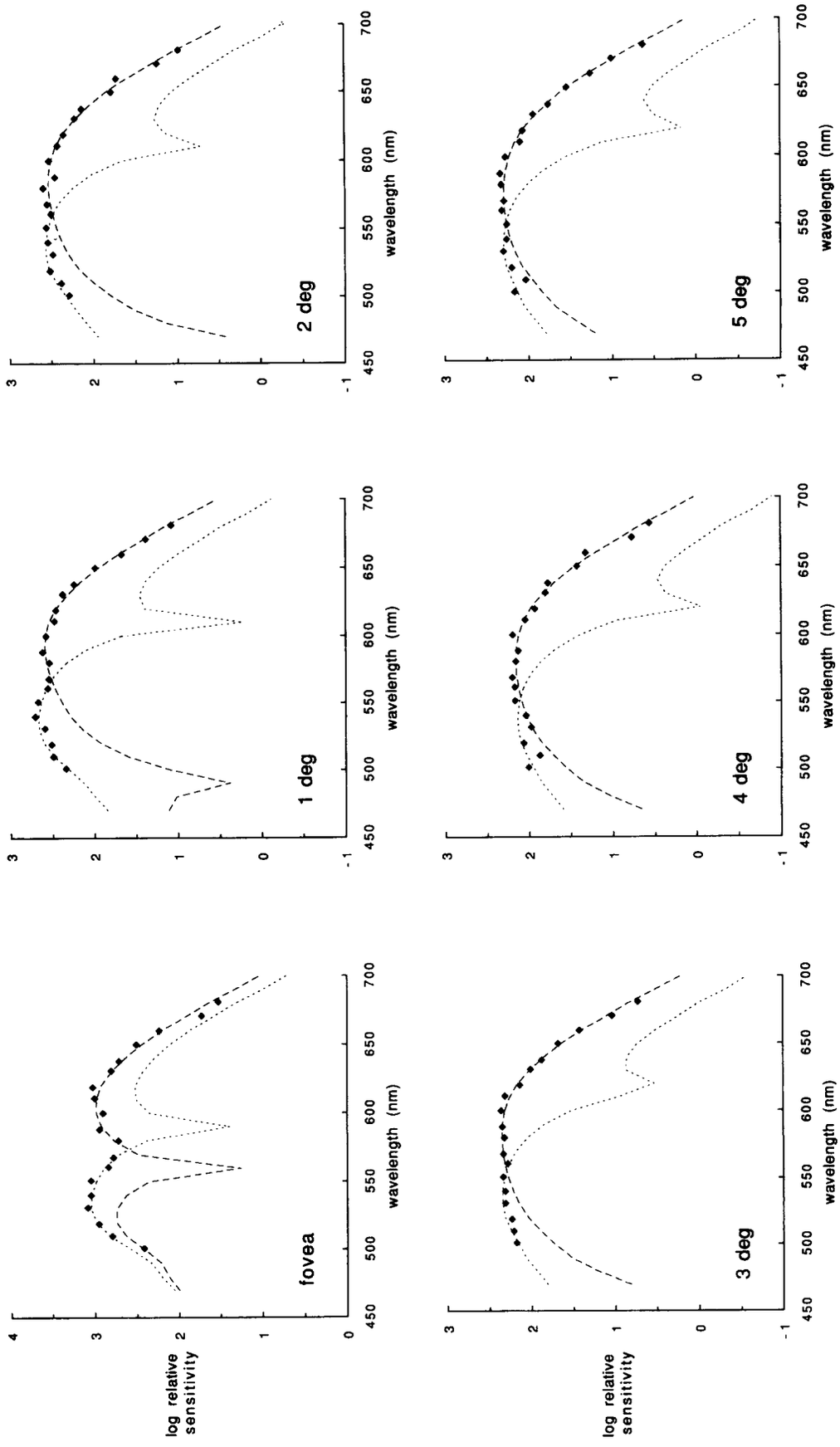

FIGURE 5. Spectral sensitivities for WV from the fovea to 5 deg eccentricity. Legend same as Fig. 4.

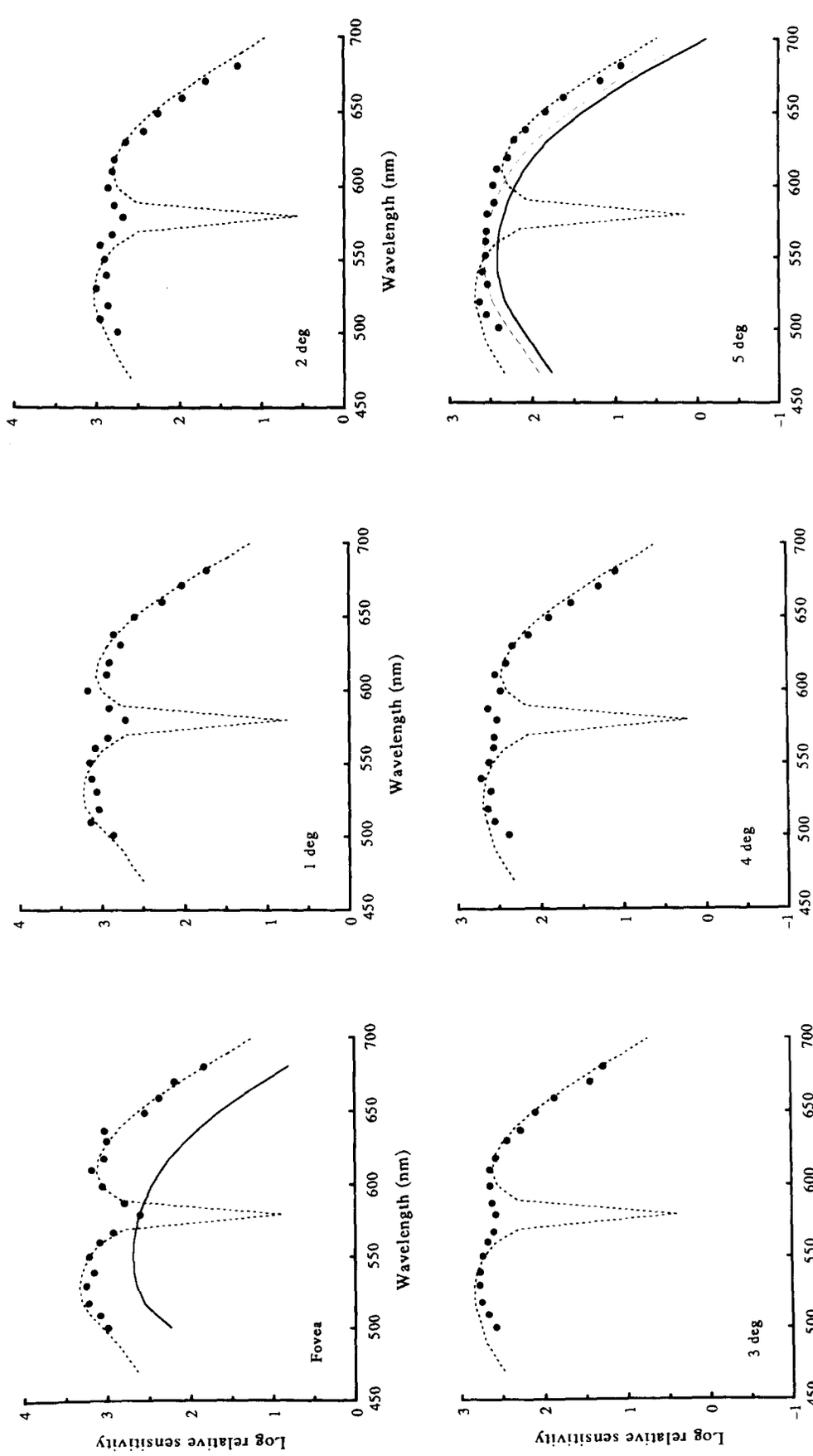

FIGURE 6. Spectral sensitivities for SH replotted from Fig. 4 fit with the single channel model, green peak $= k_1|M_z - k_2L_z|$, red peak $= k_1|M_z - k_2L_z|$. Constant k_2 determines the notch position. Coefficients k_1 and k_2 allow the green and red peaks to slide vertically independently to best fit the data (Thornton & Pugh, 1983a). The single channel model alone fails to capture the disappearing notch. The solid line on the first and last panels show the $V(\lambda)$ luminosity function correctly positioned on the ordinate by independent measurement (see Methods). The final panel also shows $V(\lambda)$ best fit by eye over the center of the spectrum (dashed line). Despite the apparently good fit of $V(\lambda)$ to the data in the last panel, our evidence shows that this scheme is incorrect.

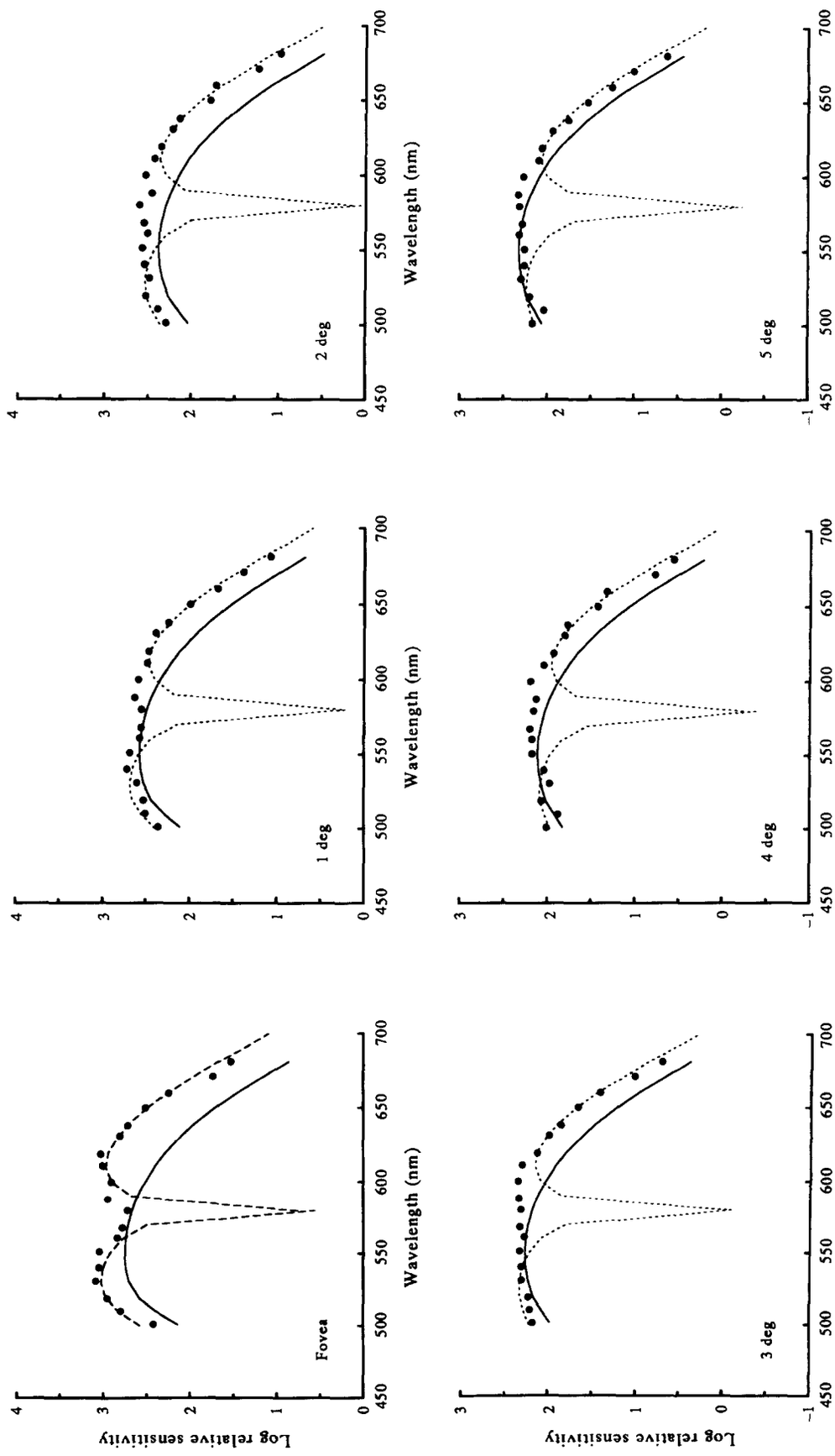

FIGURE 7. Spectral sensitivities for WV measured using a low frequency test on a white background. The dashed line indicates the best fit single channel model. The green peak is fit from 501 to 551 nm and the red peak from 600 to 681 nm. The solid line is $V(\lambda)$ correctly positioned by measurement. Inspection shows consistently poor fits in the region from 580 to 620 nm. Further evidence from discrimination experiments argues against achromatic mechanism detection over the center of the spectrum in the parafovea. Therefore we reject the model shown in this figure.

TABLE 1. Coefficients used to fit the one- and two-channel models for both subjects. Coefficients are explained in the Modeling section

	2 channel model				Single channel model		
	k_1	k_2	k_3	k_4	k_2	k_1	k_3
SH							
Fovea	3.30	1.80	3.65	0.75	0.65	3.70	3.75
1 deg	3.10	2.10	3.55	0.80	0.65	3.60	3.70
2 deg	2.65	3.10	3.10	1.10	0.65	3.40	3.45
3 deg	2.45	3.00	2.90	1.15	0.65	3.20	3.25
4 deg	2.10	4.55	2.55	1.70	0.65	3.05	3.10
5 deg	2.05	4.70	2.40	1.95	0.65	3.05	3.00
WV							
Fovea	3.05	1.90	3.40	0.90	0.65	3.40	3.60
1 deg	2.25	3.55	2.65	1.55	0.65	3.05	3.10
2 deg	2.10	3.85	2.40	2.10	0.65	2.90	3.00
3 deg	1.80	4.45	2.15	2.35	0.65	2.70	2.80
4 deg	1.50	5.30	1.95	2.40	0.65	2.45	2.60
5 deg	1.65	5.35	1.85	3.60	0.65	2.60	2.70

nonopponent, and second, where are the spectral boundaries between discriminable colors? Psychometric functions were plotted for detection and discrimination of pairs of lights at 5 deg eccentricity. Figure 11 shows 2 psychometric functions for SH, one indicating detection performance for a 570 nm test (■—■) and the other showing discrimination performance, 570 vs 590 nm, when the test was 570 nm (△- - -△). Figure 12 shows the complementary psychometric functions, indicating detection performance for a 590 nm test light (■—■), and discrimination performance, 590 vs 570 nm, when the test was 590 nm (△- - -△). We determined discrimination at 90% detectability (Mullen & Kulikowski, 1991) using a 2 × 2 forced choice procedure. Discrimination of 570 from 590 nm was 77.1%, and 590 from 570 nm was 79.5%. The mean was 78.3% (maximum possible is 90%, minimum is 50%). The 570 and 590 nm lights were discriminated by slight greenish and reddish components, respectively. These data are inconsistent with both lights being detected by the same luminance mechanism so the schemes shown in the 5 deg fits in Figs 6 and 7 must be incorrect. Further, the lack of an achromatic percept indicates neither light is detected by a luminance mechanism. Therefore, even in the notch region, where the sensitivity of a luminance mechanism is expected to be maximal relative to the chromatic mechanisms, chromatically opponent mechanisms are active. While these results rule out the possibility that an achromatic mechanism is the sole detecting mechanism, they do not rule out the possibility that there is a small achromatic contribution to detection in this region. This might help explain the less than perfect discrimination-at-threshold for all pairs of wavelengths tested. On the other hand, foveal chromatic increments tend to be a little more detectable than discriminable (King-Smith, 1975; King-Smith & Carden, 1976; Mullen & Kulikowski, 1990), and an achromatic mechanism is unlikely to contribute significantly to detection in the foveal case. Perhaps a threshold perturbation of a chromatic mechanism is insufficient to generate a color sensation. Whatever the cause of the small discrepancy, the combination of a unitary red–green mechanism and an achromatic mechanism appears unable to explain the discrimination data because the sensitivity of the unitary red–green mechanism is so low in the notch region. By reason this should lead to dominance in this spectral region by the achromatic mechanism, while we find chromatic dominance.

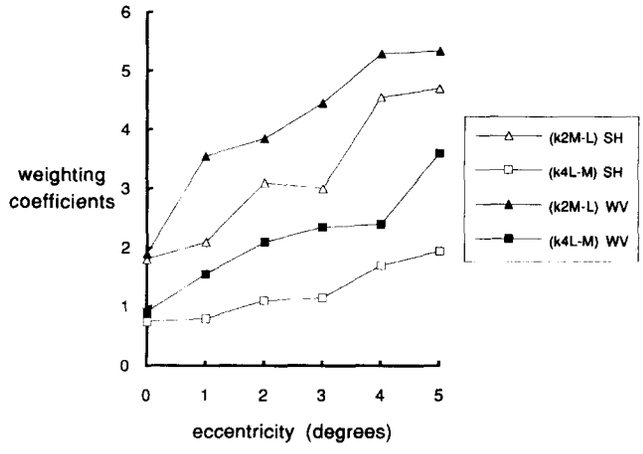

FIGURE 8. Weighting coefficients for the green–red and red–green peaks of the two channel model for each subject. Values are plotted from Table 1. For the green peak, from the fovea to 5 deg, the relative weighting of M cones increases. Similarly, for the red peak, the relative weighting of L cones increases. The relative increases are less for SH than WV indicating that the spectral sensitivity curves are more opponent away from the fovea for the former subject.

Additional detection versus discrimination experiments showed: (1) 501 nm (blue) can be discriminated from 519 nm (green) almost perfectly at 90% detection, (2) 519 nm (green) cannot be discriminated from 540 nm (green) at 90% detection, (3) 561 nm (green) and 580 nm (yellow/orange) can be discriminated in 72% of trials at 90% detection, (4) 580 nm (yellow/orange) can be discriminated from 600 nm (red) in 69% of trials at 90% detection, (5) 619 nm cannot be discriminated from 670 nm (red). The color names in parentheses were chosen by the subjects as descriptors for the color judgments. For example, 570 nm was described as green when paired with longer wavelengths even though it had a substantial yellow component. Similarly, 590 nm was described as red when paired with shorter wavelengths. Emphasizing the different colors of a pair rather than the common color component is necessary to make discrimination judgments. The color names for each wavelength are not directly comparable to the color boundaries given by Mullen and Kulikowski (1990), which are defined as wavelengths at which discrimination between adjacent spectral regions is half way between chance (50%) and perfect (90%), i.e. 70%. We are unable to precisely locate the boundaries between color sensations due to the limited wavelength pairs chosen. However, we can examine whether our data are consistent with the foveal boundaries. Foveal boundaries are at about 490, 566 and 585 nm. Our first boundary, between blue and green, is somewhere between 501 and 519 nm at 5 deg eccentricity. The different location of this boundary is not surprising given the increase in sensitivity of the "blue" mechanism away from the fovea (Castano & Sperling, 1982). We can discriminate neither 519 and

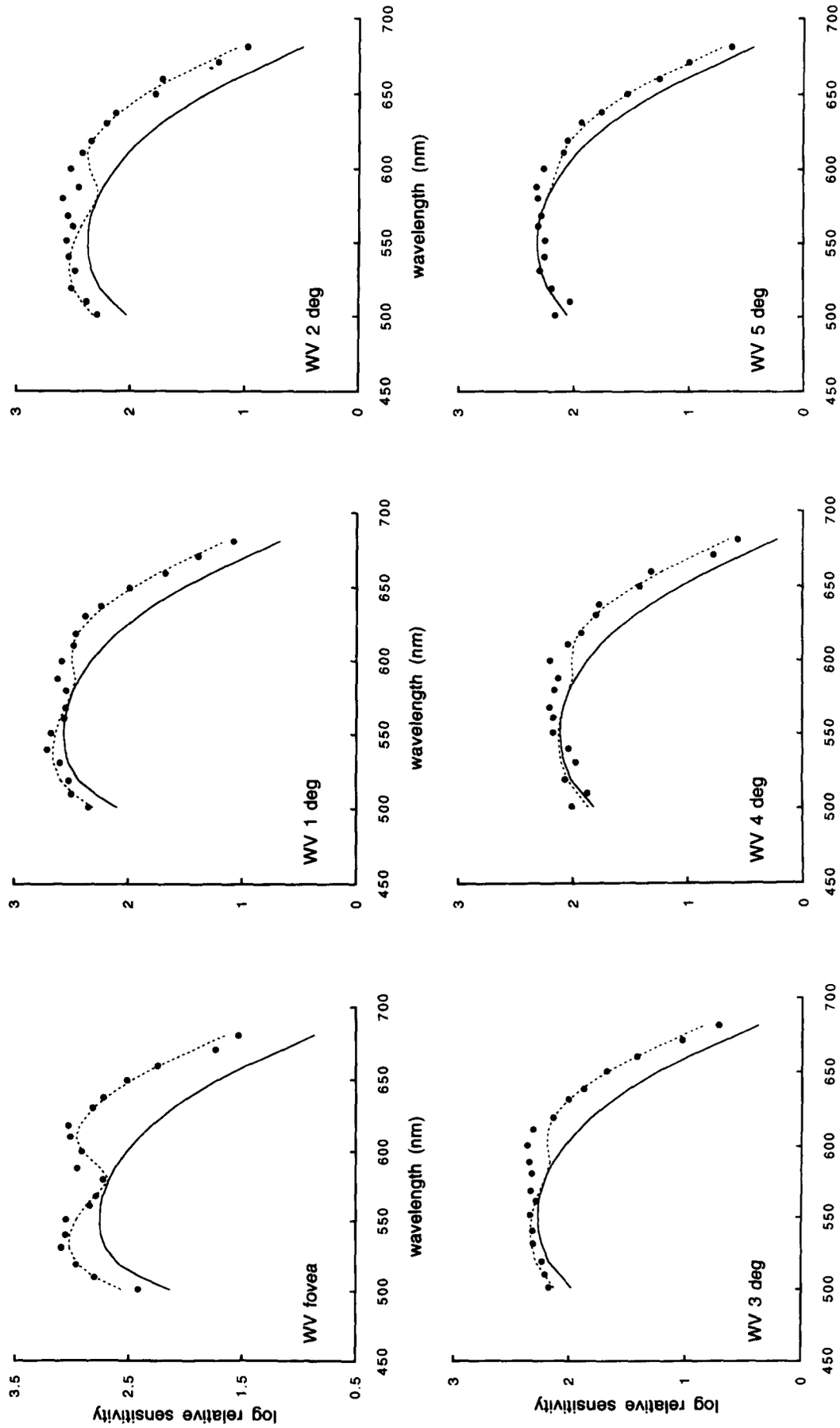

FIGURE 9. Vector model fits to spectral sensitivities for author WV. The solid line represents the photopic luminosity function $V(\lambda)$ correctly positioned by separate measurement. Clearly, the vector model fit is poor. The vector model is defined as:

$$\text{green peak}(\lambda = 500\text{–}570\text{ nm}) = [(V_\lambda)^2 + k_1(k_2 L_\lambda - M_\lambda)^2]^{0.5};$$

$$\text{red peak}(\lambda = 580\text{–}660\text{ nm}) = [(V_\lambda)^2 + k_3(k_2 L_\lambda - M_\lambda)^2]^{0.5}.$$

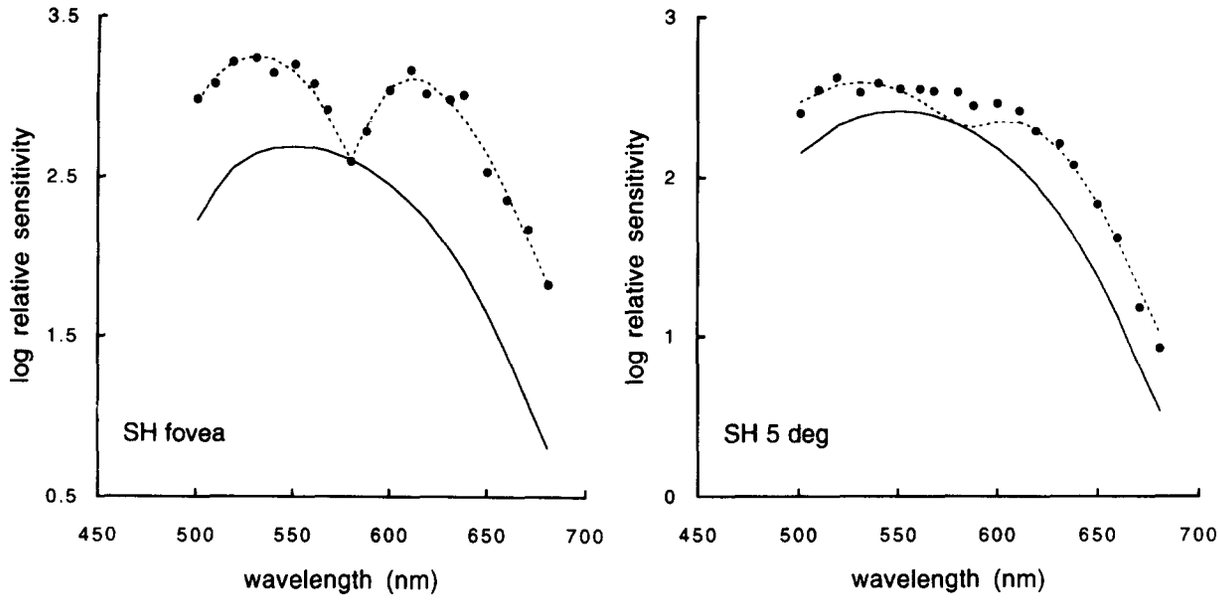

FIGURE 10. Vector model fits to SH spectral sensitivities at the fovea and 5 deg eccentricity. The poor fit at 5 deg is evident at the center of the spectrum. Legend same as Fig. 9.

540 nm, nor 619 and 670 nm, consistent with the foveal boundaries. Our data predict boundaries between 561 and 580 nm and between 570 and 590 nm, both consistent with foveal boundaries. Our discrimination of 580 and 600 nm was 69%, just below the 70% needed to predict a boundary between this pair. The 580 nm light appeared orange–yellow which might suggest the division between red and yellow is shifted from 585 nm to a slightly shorter wavelength at 5 deg eccentricity. In summary, our data are consistent with the two long wavelength boundaries found at the fovea, with the exception of slightly worse discrimination than predicted between 580 and 600 nm. This is quite remarkable in light of the change in spectral sensitivity between the two retinal positions and it leaves little doubt that chromatic mechanisms are detecting the low frequency test target used in these experiments.

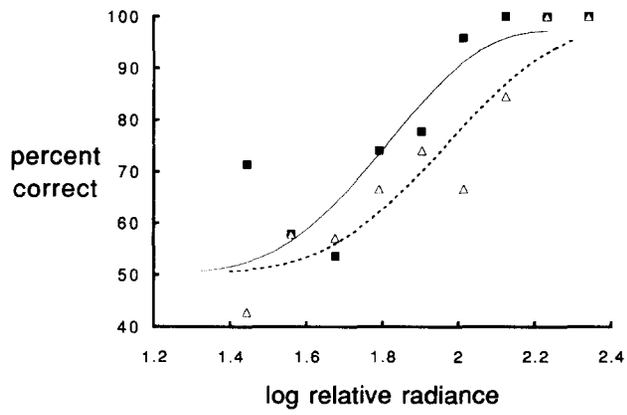

FIGURE 11. Color discrimination and detection performance for SH. Solid symbols show detection performance for a 570 nm test at 5 deg eccentricity. Open symbols show performance at discriminating the 570 nm test from a 590 nm test, measured simultaneously with the detection performance. Solid and dotted curves are the best fit probit functions to the detection and discrimination data. As might be expected, detection is slightly better than discrimination. At 90% detection, discrimination is 77.1%. The abscissa scale units are arbitrary.

Additivity experiments

Evidence presented so far indicates that color opponent mechanisms dominate detection at 5 deg eccentricity. Further evidence consistent with this is provided by additivity experiments. Components of 519 and 620 nm were presented in threshold-unit-ratios of 1:2, 1:1 and 2:1. Figure 13A shows huge failures of additivity for both subjects at the fovea, as expected (Filled symbols, SH; Open symbols, WV). The data fall outside the unit square, which indicates that the signals generated from the lights are inhibitory (Drum, 1982). Figure 13B (SH) and 13C (WV) show smaller additivity failures at 5 deg eccentricity, in the direction of subadditivity. Note the scale change. The components are more strongly subadditive for subject SH than for WV which

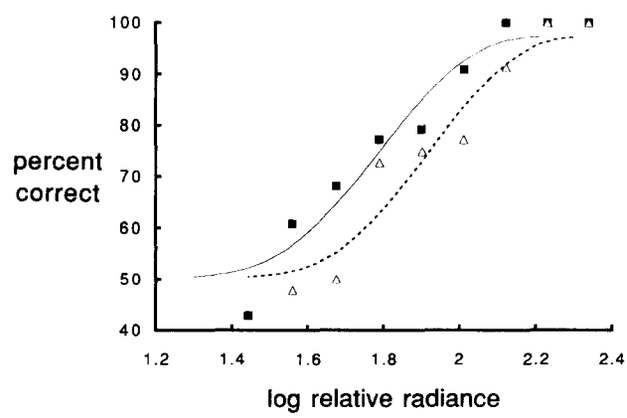

FIGURE 12. Color discrimination and detection performance for SH. Solid symbols show detection performance for a 590 nm test at 5 deg eccentricity. Open symbols show performance at discriminating the 590 nm test from a 570 nm test. At 90% detection, discrimination is 79.5%. Other details as Fig. 10.

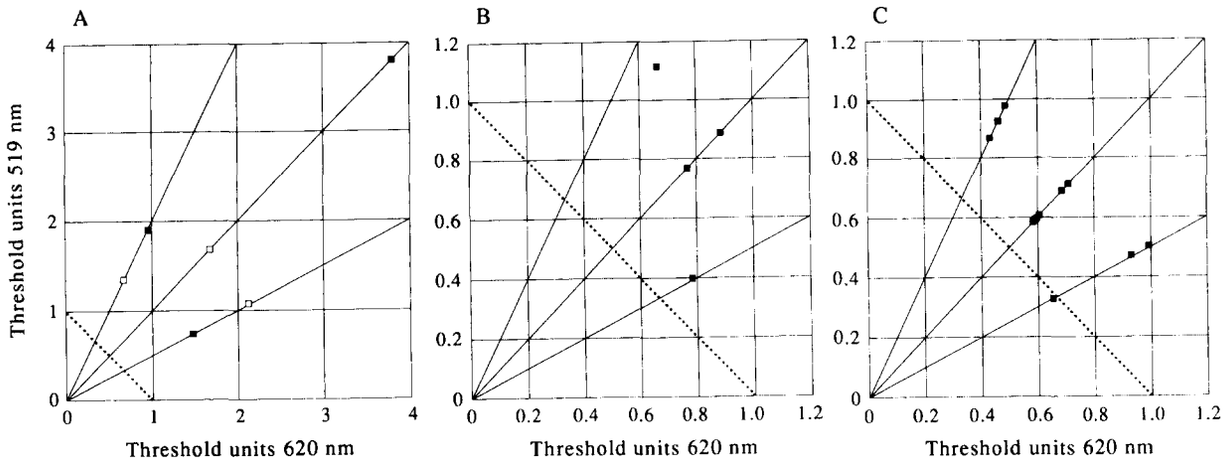

FIGURE 13. Additivity experiments. Each point is a single threshold determination generated from 50 trials of a 2AFC experiment (see Methods). (A) Huge additivity failures at the fovea for SH (solid symbols) and WV (open symbols). (B) Subadditivity for SH at 5 deg eccentricity. 13C: subadditivity for WV at 5 deg eccentricity.

is consistent with the more evident notch in the former's spectral sensitivity data at all retinal locations. The 5 deg data for both observers are most consistent with subadditivity, rather than cancellation. We can conclude from these results that the parafoveal 519 and 620 nm components are not detected by a single linear system, because the data do not fall along the additivity line. The data are consistent with an interaction between at least two mechanisms, although we cannot determine from these data the nature of the mechanisms. Specifically, we cannot exclude the possibility of an achromatic mechanism contribution. The two or more mechanisms lack complete independence and they do not demonstrate the cancellation (inhibition) that is apparent foveally. The subadditivity implies summation between two or more mechanisms, for example, probability or vector summation between L–M and M–L mechanisms. However, if these particular mechanisms are underlying the additivity data, the lack of cancellation does suggest a different combination rule for the L–M and the M–L mechanisms in the parafovea. Whatever the cause of the subadditivity, the results argue against detection by a single linear mechanism.

DISCUSSION

The main result of these experiments is that chromatically opponent mechanisms contribute strongly to detection of a small, low frequency test light in parafoveal retina, yet the spectral envelope of the detection mechanisms is unimodal. The presence of a unimodal spectral sensitivity, could lead one to conclude incorrectly that detection is by a nonopponent mechanism, such as $V(\lambda)$ or L cones, over at least part of the spectrum. Moreover, if a single channel model of opponent processing is chosen to fit the data, there is a temptation to fit the middle part of the spectrum with a luminance mechanism (see Figs 6 and 7), and conclusions about the relative sensitivities of opponent and nonopponent mechanisms (or P and M pathways) may be made in error. In single unit physiology and in psychophysical experiments on animals or patients, it is often impractical or impossible to use measures of color detection and discrimination to distinguish between opponent and nonopponent detection mechanisms. In these types of experiment caution is needed in interpreting "composite" spectral curves, and the *a priori* assumption that independent chromatic and achromatic mechanisms can be manipulated to best fit the data needs to be critically examined for the particular stimulus condition used (Harwerth, Smith & DeSantis, 1993; Crook, Lee, Tigwell & Valberg, 1987). As we have shown, a fortuitously good fit to the data can be achieved using an incorrect model. The failure of independent opponent and nonopponent mechanisms, and of a vector model, to account for the data under our stimulus conditions does not necessarily mean that these models are inappropriate at further retinal eccentricities, or using different stimuli. Regardless of which model is used to describe the data, empirical justification is needed.

The evidence presented here indicates that color opponent mechanisms detect the test light at all retinal locations from the fovea to 5 deg eccentricity, except perhaps at the low point of the spectral notch. In general, previous studies indicate that as a fixed size test light stimulates further eccentric retinal points, chromatic sensitivity diminishes relative to achromatic sensitivity, leading to the notion the central retina specializes in color vision. For example, color contrast sensitivity declines more rapidly than luminance contrast sensitivity across the visual field (Mullen, 1991) and colored targets appear achromatic in the peripheral visual field but their color can be identified as the target approaches the fovea (Pokorny, Smith, Verriest & Pinkers, 1979). Also consistent with this specialization is the increase in the relative density of P (P_β) ganglion cells relative to M (P_α) as the fovea is approached (Perry, Oehler & Cowey, 1984). These results, taken literally, can suggest the wrong interpretation of a unimodal spectral sensitivity. Direct measurements of additivity, appearance, threshold discrimination and so on, made using the same stimulus as the spectral sensitivity, are powerful tools

with which to differentiate between opponent and nonopponent detection mechanisms.

Relationship to physiology

How is our changing spectral sensitivity related to changes in properties of retinal neurons across the parafovea? We assume that the relative numbers of M and L cones and their absorption spectra do not change as a function of eccentricity (Nerger & Cicerone, 1992). We further assume that +M–L ganglion cells, i.e. M cones feeding receptive field (RF) centers in an excitatory manner and L cones feeding the RF surrounds in an inhibitory manner, detect increments from 500 to approximately 570 nm, and that +L–M ganglion cells detect from approximately 580–680 nm [because we are dealing with color, we have limited our attention to the P stream, even though the M stream has weak opponency (Derrington, Krauskopf & Lennie, 1984; Kaplan, Shapley & Purpura, 1989)]. Dendritic fields of P_β ganglion cells within 5 deg of macaque monkey fovea, are less than 10 μm in diameter, which is equivalent to approximately 2.5 min arc (Perry *et al.*, 1984). Based on the resolution ability of macaque P_β ganglion cells, and the theoretical RF center size needed to support this resolution, Crook, Lange-Malecki, Lee and Valberg (1988) have estimated that RF center size must exceed the dendritic tree size by a factor of 4 or 5. Thus monkey RF size within the central 5 deg is expected to be less than 12.5 min arc diameter, less than half the diameter of our test spot. Others have directly measured RF center sizes, and suggest they are even smaller than this, ranging from 2.4 to 5.4 arc min diameter (DeMonasterio, 1978). Therefore, our test fills RF centers at all eccentricities measured. While there are several studies documenting the RF center sizes of ganglion and lateral geniculate nucleus (LGN) cells in monkeys, or their resolving abilities (Hubel & Wiesel, 1960; Wiesel & Hubel, 1966; DeMonasterio & Gouras, 1975; DeMonasterio, 1978; Derrington & Lennie, 1984; Blakemore & Vital-Durand, 1986) systematic measurements of total RF size as a function of eccentricity are lacking. DeMonasterio (1978) measured surround profiles ranging from 0.2 to 1.2 deg within the central 20 deg of macaque retina, but these may be underestimates because, as he points out, chromatic adaptation used to desensitize the center mechanism will also desensitize the surround to some extent. Recent evidence, however, suggests that center and surrounds may be almost coextensive in P ganglion cells (Shapley, Reid & Kaplan, 1991). Given there is no clear consensus on surround or total RF size in the physiology literature, it is difficult to know whether our test fills the entire RF at each eccentricity. However, even at 5 deg eccentricity, our test probably covers most of the RF and the more peripheral regions of the RF surround that may be left uncovered are unlikely to be capable of significantly changing the degree of spectral opponency of the cell. Therefore, assuming quantitative similarities between macaque and human ganglion cells, the change in cone balance of the green–red and red–green psychophysical mechanisms from fovea to 5 deg eccentricity (approximately 2M:L to 5M:L for the green–red and 0.8L:M to 2.8L:M for red–green) does not reflect sampling different extents of P ganglion cell RF's. It must reflect either a change in connectivity that causes ganglion cell center mechanisms to become relatively more dominant parafoveally, or it reflects changes beyond the retina.

A few studies have looked at changing center/surround balance with eccentricity in P ganglion cells. Using stimuli that filled the entire RF, Zrenner and Gouras (1983) reported that all degrees of cone dominance are seen at all retinal locations from 0 to 8 deg eccentricity. Spectral crosspoints (from excitation to inhibition in response to spectral increments) varied for red/green opponent cells from 480 to 630 nm. At the fovea most cells have relatively balanced antagonistic inputs from M and L cones, while between 4 and 8 deg the most commonly encountered cells were those dominated by excitatory L cone input to the RF center (Zrenner & Gouras, 1983). Cells that would presumably correspond to the green peak of the psychophysical function, i.e. cells dominated by +M cone input to the RF center, were rarely encountered between 4 and 8 deg. This raises a problem with associating these ganglion cell data with our psychophysical data.

In contrast to the wide variety of weightings for ganglion cells, parvo-LGN cells have fairly balanced inputs from L and M cones (Derrington *et al.*, 1984), with much smaller variations in spectral crosspoints within a class of cells than suggested for ganglion cells (DeValois, Abramov & Jacobs, 1966). This makes parvo-LGN cells good candidates for modeling foveal psychophysical opponent spectral sensitivity curves, provided that blue–yellow cells are ignored. However, at 5 deg eccentricity where the spectral sensitivity no longer has a deep notch, an envelope of most sensitive red–green parvo-LGN cells underestimates sensitivity in the notch region. Thus the spectral sensitivity of parvo-LGN cells alone cannot account for the parafoveal data. This was shown nicely by Crook *et al.* (1987), who measured a notchless human spectral sensitivity on a white field at 10 deg eccentricity using a 4 deg test spot. The upper envelope of macaque parvo-LGN cells fit to this spectral curve significantly underestimated sensitivity across a wide spectral region centered around 570 nm. The authors therefore fit this middle part of the spectrum with a luminance mechanism (defined by the spectral sensitivity of magno-LGN cells). The luminance mechanism provided a good fit to the physiological data, but no further support was provided for a nonopponent detection mechanism. As we argue here, if more than one model is capable of fitting a spectral sensitivity curve, the *a priori* choice of model dictates how the data are interpreted.

Cortical cells in V1 show a much wider range of L to M cone weighting in their inputs than parvo–LGN cells (Lennie, Krauskopf & Sclar, 1990). Simple and complex cells tend to be dominated by either L cones (for +L–M cells) or M cones (for +M–L cells), rather than having a balanced input (Lennie *et al.*, 1990). It is possible that

an envelope of the most sensitive cortical opponent cells could fit the psychophysical spectral sensitivity of Crook *et al.* (1987), and our extrafoveal curves, without involving nonopponent cells. To account for the psychophysics, cortical cells with foveal RF's would need balanced cone weightings while cells with parafoveal RF's would need progressively more center dominated cone inputs. It is unknown whether the population changes in this manner because responses reported in the literature tend to be pooled over the relatively restricted retinal area tested in our psychophysical experiments.

In summary so far, our test probably fills both the center and the surround of P retinal ganglion cells at least to 5 deg eccentricity, and therefore differential stimulation of center and surround at different eccentricities is unlikely to account for the spectral sensitivity changes we report. P ganglion cells show a variety of center/surround balances but the balances change systematically with eccentricity in a fashion that cannot account for our spectral sensitivities. LGN parvo-cell center and surround balances are approximately equal, and the upper envelope of their sensitivities predicts a notch in the yellow spectral region. However, the notch is absent in our spectral sensitivities, and LGN cells fail to capture this feature. The earliest cells with appropriate cone weightings are probably in striate cortex.

Relationship to previous psychophysics

Finkelstein and Hood (1982, 1984) and Hood and Finkelstein (1983) studied the detection and appearance of small, brief test lights on a white field at the fovea. They demonstrated that the small test was detected by a mechanism with a nonopponent looking, unimodal spectral sensitivity curve, but that the flashed field sensitivity showed strong opponent mechanism input. Furthermore they showed that opponent mechanisms are implicated in the detection of the test lights (Finkelstein & Hood, 1984; Kaiser & Ayama, 1986). Our results can be thought of as analogous to these results because reducing the size of a foveal test light alters spectral sensitivity in a similar way to moving a constant size test onto the parafoveal retina. Finkelstein and Hood proposed a "variable tuning" hypothesis to account for the change in opponent spectral sensitivity caused by reducing the test size and duration. In their scheme, the psychophysical spectral sensitivity is thought to parallel changes in the spectral tuning of individual opponent cells as test size is changed. We have argued above that variable tuning of ganglion cells is unlikely to account for our data, because our stimulus fills P ganglion cell RFs at all locations tested (assuming quantitative similarities between human and macaque cells). However, cortical cells (from Areas 17, 18 and V4) have been shown to change their spectral tuning as stimulus size changes (Kruger & Gouras, 1980), and the dimensions over which stimulus tuning occurs appear more compatible with our psychophysics. As stimulus size increases, sensitivity of a cell to the spectral extremes increases relative to the mid-spectrum, as required. Thus, the variable tuning of cortical opponent cells might play a role in the spectral sensitivity changes reported here.

It should be noted that the similarities in the changes in spectral sensitivity due to reducing test size at the fovea and moving a constant size test to extrafoveal retina, might be coincidental. Variable tuning of opponent cells at some level of the visual pathways might explain the variable-size test, fixed location data (Finkelstein & Hood, 1984), but changes in RF properties or in populations of cells away from the fovea might explain the fixed-size test, variable location data presented here. Of course, at an extraretinal level, a combination of somewhat larger RFs at 5 deg with more center dominated responses could account for our data.

Our data show that the notch at approximately 580 nm reduces in depth as eccentricity increases and while we have argued that the mechanism detecting in this spectral region is not a luminance channel, we have not addressed the possibility of detection by the yellow lobe of a blue/yellow chromatic process. The striking absence of a yellow peak at the fovea under neutral adaptation conditions that strongly favor opponent detection mechanisms, reflects a fundamental insensitivity of blue–yellow processing in the notch spectral region under these stimulus conditions. Perhaps the spectral sensitivities under neutral adaptation reflect visual processing prior to the elaboration of yellow signals, just as other threshold psychophysical paradigms can tap into visual processing at different levels (Teller, 1980). Previous studies using foveal lights have commented on the lack of need for a yellow peak of a blue–yellow opponent process in increment threshold data (Sperling & Harwerth, 1971; Kranda & King-Smith, 1979). Two features of the current data suggest to us that detection over the center spectrum is not by a yellow mechanism operating in an upper envelope mode. First, the color discrimination of 570 and 590 nm at threshold at 5 deg eccentricity, and the respective greenish and reddish appearances, suggest different detection mechanisms for these lights. Therefore, a yellow mechanism, if present, must lie within these limits. Given these discrimination results, it is unlikely that a yellow mechanism detects test lights from 560 to 600 nm, the spectral region occupied by $V(\lambda)$ in Figs 6 and 7 (last panels). Second, inspection of SH's data, in particular the spectral sensitivities at 1 and 2 deg eccentricity (Fig. 6) indicates that positioning a yellow mechanism at the low point of the notch, will result in a poor fit to the data points that lie between the notch minimum and the maxima at the green and red peaks. This is because the notch reduces in depth and its sides get progressively shallower with eccentricity. Together, these points argue against an upper envelope model for detection in the parafovea comprised of a blue–yellow channel and a unitary red–green channel.

In summary, we have shown systematic changes in spectral sensitivity on a white field as a small test is moved from the fovea to 5 deg eccentricity. Opponent mechanisms are active in detection across the spectrum at all retinal locations and the spectral sensitivity curve can be described well by a model having two

red/green opponent channels, M–L and L–M (Sperling & Harwerth, 1971). Away from the fovea, the red peak becomes more dominated by L cones and the green peak by M cones, thereby reducing the depth of Sloan's notch, and making the sides of the notch more shallow. This change in cone weightings may occur cortically. Although an upper envelope model with a single red–green channel and a nonopponent channel might appear to provide a reasonable fit for the detection data, it is probably incorrect because, across a wide region of the spectrum, it fails to predict color discrimination at threshold. A vector model combining signals from a luminance channel and a single red/green channel poorly describes the spectral sensitivity data in the center of the spectrum. These results therefore argue against a unitary red/green process in which both positive and negative responses contribute to detection. Instead, our favored model allows detection by positive responses only, and it allows the mechanisms that detect green and red increments to differ in cone weightings (Sperling & Harwerth, 1971). We have attempted to compare three simple models developed previously for use at the fovea, to determine which is most consistent with the extrafoveal data. Although the two channel model is more consistent than the other models with the extrafoveal data and it accurately fits the spectral sensitivity curves, the addition of more mechanisms, such as an achromatic mechanism, might further improve the model's ability to fully account for the additivity data, and perhaps the discrimination at threshold results. The adoption of two red/green opponent channels to account for our data suggests that the mechanism of red–green chromatic processing is not unitary. A similar conclusion has been reached by others using different approaches (DeValois & DeValois, 1993; DeValois, Switkes & DeValois, 1994; Smith, Glennie & Pokorny, 1994).

To fit our parafoveal threshold data, we have used three models. If more than one model is capable of adequately fitting the data on a least squares criterion, then this criterion alone is insufficient to choose one model over another. The finally adopted model needs validating by separate criteria, as we have attempted to show here. We believe this is particularly important because these models are mechanistic and the choice of model dictates the data interpretation. Therefore whenever spectral sensitivities are modified by the effects of age, pathology, eccentricity or other stimulus parameters, the chosen model needs evaluating using factors in addition to the model's ability to describe shape changes in spectral sensitivity.

REFERENCES

Abramov, I., Gordon, J. & Chan, H. (1991). Color appearance in the peripheral retina: effects of stimulus size. *Journal of the Optical Society of America, 8*, 404–414.

Blakemore, C. & Vital-Durand, F. (1986). Organization and post-natal development of the monkey's lateral geniculate nucleus. *Journal of Physiology, 380*, 453–491.

Castano, J. A. & Sperling, H. G. (1982). Sensitivity of the blue-sensitive cones across the central retina. *Vision Research, 22*, 661–673.

Crook, J. M., Lange-Malecki, B., Lee, B. B. & Valberg, A. (1988). Visual resolution of Macaque retinal ganglion cells. *Journal of Physiology, London, 396*, 205–224.

Crook, J. M., Lee, B. B., Tigwell, D. A. & Valberg, A. (1987). Thresholds to chromatic spots of cells in the Macaque geniculate nucleus as compared to detection sensitivity in man. *Journal of Physiology, London, 392*, 193–211.

DeMonasterio, F. M. (1978). Center and surround mechanisms of opponent-color X and Y ganglion cells of retina of Macaques. *Journal of Neurophysiology, 41*, 1418–1434.

DeMonasterio, F. M. & Gouras, P. (1975). Functional properties of ganglion cells of the Rhesus monkey retina. *Journal of Physiology, 251*, 167–195.

Derrington, A. M. & Lennie, P. (1984). Spatial and temporal contrast sensitivities of neurons in lateral geniculate nucleus of Macaque. *Journal of Physiology, 357*, 219–240.

Derrington, A. M., Krauskopf, J. & Lennie, P. (1984). Chromatic mechanisms in lateral 3 geniculate nucleus of Macaque. *Journal of Physiology, 57*, 241–265.

DeValois, R. L. & DeValois, K. K. (1993). A multi-stage color model. *Vision Research, 33*, 1053–1065.

DeValois, R. L., Abramov, I. & Jacobs, G. H. (1966). Analysis of response patterns of LGN cells. *Journal of the Optical Society of America, 56*, 966–977.

DeValois, R. L., Switkes, E. & DeValois K. K. (1994). Peripheral unidirectional color contrast sensitivity. *Investigative Ophthalmology and Visual Science, 35 (Suppl.)*, 1409.

Drum, B. (1982). Summation of rod and cone responses at absolute threshold. *Vision Research, 22*, 823–826.

van Esch, J. A., Koldenhof, E. E., van Doorn, A. J. & Koenderink, J. J. (1984). Spectral sensitivity and wavelength discrimination of the human peripheral visual field. *Journal of the Optical Society of America, 1*, 443–450.

Finkelstein, M. A. & Hood, D. C. (1982). Opponent-color cells can influence detection of small, brief lights. *Vision Research, 22*, 89–95.

Finkelstein, M. A. & Hood, D. C. (1984). Detection and discrimination of small, brief lights: variable tuning of opponent channels. *Vision Research, 24*, 175–181.

Finney, D. J. (1947). *Probit analysis, a statistical treatment of the sigmoid response curve*. Cambridge University Press.

Gordon, J. & Abramov, I. (1977). Color vision in the peripheral retina. II. Hue and saturation. *Journal of the Optical Society of America, 67*, 202–207.

Guth, S. L. (1991). Model for color vision and light adaptation. *Journal of the Optical Society of America, 8*, 976–993.

Guth, S. L., Donley, N. J. & Marrocco, R. T. (1969). On luminance additivity and related topics. *Vision Research, 9*, 537–575.

Guth, S. L., Massof, R. W. & Benzschawel, T. (1980). Vector model for normal and dichromatic color vision. *Journal of the Optical Society of America, 70*, 197–212.

Harwerth, R. S., Smith, E. L. & DeSantis, L. (1993). Mechanisms mediating visual detection in static perimetry. *Investigative Ophthalmology and Visual Science, 34*, 3011–3023.

Hood, D. C. & Finkelstein, M. A. (1983). A case for the revision of textbook models of color vision: The detection and appearance of small, brief lights. In Mollon, J. D. & Sharpe, L. T. (Eds) *Colour vision, physiology and psychophysics* (pp. 385–398). London: Academic Press.

Hubel, D. H. & Wiesel, T. N. (1960). Receptive fields of optic nerve fibres in the Spider monkey. *Journal of Physiology, 154*, 572–580.

Johnson, M. A. & Massof, R. W. (1982). The effects of stimulus size on chromatic thresholds in peripheral retina. In Verriest, G. (Ed.) *Colour vision deficiencies VI* (pp. 15–18). The Hague: Junk.

Johnson, M. A. (1986). Color vision in the peripheral retina. *American Journal of Optometry and Physiological Optics, 63*, 97–103.

Kaiser, P. K. & Ayama, M. (1986). Small, brief foveal stimuli: an additivity experiment. *Journal of the Optical Society of America, 7*, 930–934.

Kaplan, E., Shapley, R. M. & Purpura, K. (1989). Spatial and spectral mechanisms of primate retinal ganglion cells. In Kulikowski, J. J.,

Dickinson, C. M. & Murray, I. J. (Eds) *Seeing contour and colour* (pp. 36–40). Oxford: Pergamon Press.

Kelly, D. H. (1983) Spatiotemporal variation of chromatic and achromatic contrast thresholds. *Journal of the Optical Society of America, 73*, 742–750.

King-Smith, P. E. (1975). Visual detection analysed in terms of luminance and chromatic signals. *Nature, 255*, 69–70.

King-Smith, P. E. & Carden, D. (1976). Luminance and opponent-color contributions to visual detection and adaptation and to temporal and spatial integration. *Journal of the Optical Society of America, 66*, 709–717.

Kranda, K. & King-Smith, P. E. (1979). Detection of coloured stimuli by independent linear systems. *Vision Research, 19*, 733–745.

Krastel, H., Jaeger, W., Zimmermann, S., Heckmann, B. & Krystek, M. (1991). Systematics of human photopic spectral sensitivity. In Drum, B., Moreland, J. D. & Serra, A. (Eds) *Colour vision deficiencies X* (pp. 323–339). Dordrecht: Kluwer.

Kruger, J. & Gouras, P. (1980). Spectral selectivity of cells and its dependence on slit length in monkey visual cortex. *Journal of Neurophysiology, 43*, 1055–1069.

Kuyk, T. K. (1982). Spectral sensitivity of the peripheral retina to large and small stimuli. *Vision Research, 22*, 1293–1297.

Lennie, P., Krauskopf, J. & Sclar, G. (1990). Chromatic mechanisms in striate cortex of Macaque. *Journal of Neuroscience, 10*, 649–669.

Lewis, A. L., Katz, M. & Oehrlein, C. (1982). A modified achromatizing lens. *American Journal of Optometry and Physiological Optics, 59*, 909–911.

Mollon, J. D. (1982). Color vision. *Annual Review of Psychology, 33*, 41–85.

Mullen, K. T. (1991). Colour vision as a post-receptoral specialization of the central visual field. *Vision Research, 31*, 119–130.

Mullen, K. T. & Kulikowski, J. J. (1990). Wavelength discrimination at detection threshold. *Journal of the Optical Society of America, 7*, 733–743.

Nerger, J. L. & Cicerone, C. M. (1992). The ratio of L-cones to M-cones in the human parafoveal retina. *Vision Research, 32*, 879–888.

Perry, V. H., Oehler, R. & Cowey, A. (1984). Retinal ganglion cells that project to the dorsal lateral geniculate nucleus in macaque monkey. *Neuroscience, 12*, 1110–1123.

Pokorny, J., Smith, V. C., Verriest, G. & Pinkers, A. J. L. G. (1979). *Congenital and acquired color vision defects* (pp. 174–181). New York: Grune & Stratton.

Shapley, R., Reid, R. C. & Kaplan, E. (1991). Spatial pattern of cone inputs to P and M cells in monkey retina and LGN. *Investigative Ophthalmology and Visual Science, 32 (Suppl. 4)*, 1115.

Smith, V. C., Glennie, L. & Pokorny, J. (1994). Color discrimination and color appearance in the equiluminant plane. *Investigative Ophthalmology and Visual Science, 35 (Suppl.)*, 4219.

Sperling, H. G. & Harwerth, R. S. (1971). Red–green cone interactions in the increment-threshold spectral sensitivity of primates. *Science, 172*, 180–184.

Sperling, H. G., Wright, A. A. & Mills, S. L. (1991). Color vision following intense green light exposure: data and a model. *Vision Research, 31*, 1797–1812.

Stabell, U. & Stabell, B. (1984). Color-vision mechanisms of the extrafoveal retina. *Vision Research, 24*, 1969–1975.

Stromeyer, C. F., Kronauer R. E. & Cole, G. R. (1983). Adaptive mechanisms controlling sensitivity to red-green chromatic flashes. In Mollon, J. D. & Sharpe, L. T. (Eds) *Colour vision, physiology and psychophysics* (pp. 313–330). London: Academic Press.

Teller, D. Y. (1980). Locus questions in visual science. In Harris, C. S. (Ed.) *Visual coding and adaptability* (pp. 151–176). New Jersey: Erlbaum.

Thornton, J. E. & Pugh, E. N. (1983a). Red/green color opponency at detection threshold. *Science, 219*, 191–193.

Thornton, J. E. & Pugh, E. N. (1983b). Relationship of opponent colors cancellation measurements to cone-antagonistic signals deduced from increment threshold data. In Mollon, J. D. & Sharpe, L. T. (Eds) *Colour vision, physiology and psychophysics* (pp. 361–373). London: Academic Press.

Wandell, B. A., Sanchez, J. & Quinn, B. (1982). Detection/discrimination in the long wavelength pathways. *Vision Research, 22*, 1061–1069.

Watson, A. B. & Robson, J. G. (1981). Discrimination at thresholds: labeled detectors in human vision. *Vision Research, 21*, 1115–1122.

Westheimer, G. (1966). The Maxwellian view. *Vision Research, 6*, 669–682.

Wiesel, T. N. & Hubel, D. H. (1966). Spatial and chromatic interactions in the lateral geniculate body of the Rhesus monkey. *Journal of Neurophysiology, 29*, 1115–1156.

Wooten, B. R. & Wald, G. (1973). Color-vision mechanisms in the peripheral retinas of normal and dichromatic observers. *Journal of General Physiology, 61*, 125–145.

Wyszecki, G. & Stiles, W. S. (1982). *Color science: concepts and methods, quantitative data and formulae*. New York: Wiley.

Zrenner, E. & Gouras, P. (1983). Cone opponency in tonic ganglion cells and its variation with eccentricity in Rhesus monkey retina. In Mollon, J. D. & Sharpe, L. T. (Eds) *Colour vision, physiology and psychophysics* (pp. 211–223). London: Academic Press.

Acknowledgements—Supported by NSF grant BNS-8709339 and NEI grant EY07345 to GHP. We wish to thank Smith-Kettlewell Eye Research Foundation for use of the Maxwellian view optical system.